

# Engineering Notes

ENGINEERING NOTES are short manuscripts describing new developments or important results of a preliminary nature. These Notes cannot exceed 6 manuscript pages and 3 figures; a page of text may be substituted for a figure and vice versa. After informal review by the editors, they may be published within a few months of the date of receipt. Style requirements are the same as for regular contributions (see inside back cover).

## Testing a Low Reynolds Number $k$ - $\epsilon$ Turbulence Model Based on Direct Simulation Data

V. Michelassi,\* W. Rodi,† and J. Zhu‡  
University of Karlsruhe, 7500 Karlsruhe, Germany

### I. Introduction

THE  $k$ - $\epsilon$  model is mostly used in conjunction with the so-called wall functions, in which the viscosity-affected near-wall region is bridged with empirical relations based on the assumptions of a logarithmic velocity profile, local equilibrium of turbulence, and a constant near-wall stress layer. For a number of practically relevant flows, e.g., transitional, strongly accelerated (relaminarizing), and separating flows, these assumptions lose their validity. To allow a resolution of the near-wall zone, low-Reynolds-number versions of the  $k$ - $\epsilon$  model have been developed by introducing damping functions and extra terms to account for the observed near-wall effects.<sup>1</sup> Because of a lack of reliable experimental data, these near-wall modifications have largely been based on dimensional reasoning, intuition, and indirect testing. A closer look reveals that even the more established models fail to reproduce the near-wall flow characteristics in detail, as will be shown later in this Note. Direct numerical simulation (DNS) data now available enable a direct and much more thorough assessment of near-wall models. Recently, Rodi and Mansour,<sup>2</sup> hereafter referred to as RM, have evaluated the DNS channel flow data of Kim et al.<sup>3</sup> and Kim<sup>4</sup> and the zero-pressure-gradient boundary-layer data of Spalart<sup>5</sup> and deduced new forms for the eddy-viscosity damping function and for the near-wall source/sink terms in the modeled  $\epsilon$  equation. The purpose of the present Note is to use and test these proposals in actual calculations of channel and boundary-layer flows and to fine tune the model functions by comparison with the DNS data. A more detailed account is given in Ref. 6.

### II. Low Reynolds Number $k$ - $\epsilon$ Modeling

The  $k$ - $\epsilon$  model employs the eddy-viscosity concept, and for the various low  $Re$   $k$ - $\epsilon$  models the relations determining the eddy viscosity  $\nu_t$  can be written for  $2D$  shear layers in the following form:

$$\nu_t = c_\mu f_\mu \frac{k^2}{\epsilon} \quad (1)$$

$$\frac{Dk}{Dt} = \frac{\partial}{\partial y} \left[ \left( \nu + \frac{\nu_t}{\sigma_k} \right) \frac{\partial k}{\partial y} \right] + \underbrace{\nu_t \left( \frac{\partial u}{\partial y} \right)^2}_{P_k} - \epsilon \quad (2)$$

Received April 25, 1992; revision received Feb. 8, 1993; accepted for publication Feb. 9, 1993. Copyright © 1993 by the American Institute of Aeronautics and Astronautics, Inc. All rights reserved.

\*Assistant Professor, Institute for Hydromechanics, Kaiserstrasse 12; on leave from the University of Florence, Florence, Italy.

†Professor, Institute for Hydromechanics, Kaiserstrasse 12. Member AIAA.

‡Research Fellow, Institute for Hydromechanics; currently at ICOMP, Cleveland, Ohio.

$$\frac{D\epsilon}{Dt} = \underbrace{\frac{\partial}{\partial y} \left[ \left( \nu + \frac{\nu_t}{\sigma_\epsilon} \right) \frac{\partial \epsilon}{\partial y} \right]}_{\text{Diff}_\epsilon} + \underbrace{c_{\epsilon 1} f_1 \frac{\epsilon}{k} P_k}_{P_\epsilon} - \underbrace{c_{\epsilon 2} \frac{\epsilon^2}{k}}_{D_\epsilon} + E \quad (3)$$

where  $\tilde{\epsilon} = \epsilon - D$  and the various models differ through the use of different functions  $f_\mu$ ,  $f_1$ , and  $f_2$  and different terms  $D$  and  $E$ . In Eq. (1),  $c_\mu$  is a constant coefficient and  $f_\mu$  is a damping function. Some models use as turbulence time scale  $k/\epsilon$  and solve an equation for  $\epsilon$  whereas others use  $k/\tilde{\epsilon}$  and solve an equation for the isotropic dissipation rate  $\tilde{\epsilon}$ , which, in contrast to  $\epsilon$ , goes to zero at the wall. In the latter case all  $\epsilon$  in Eq. (3) should be replaced by  $\tilde{\epsilon}$ . The function  $f_2$  in the  $\epsilon$  equation is effective only very close to the wall and is generally composed of two parts

$$f_2 = f_2^1 \cdot f_2^2 \quad (4)$$

Part  $f_2^1$  simulates the change in the decay rate of homogeneous turbulence as the Reynolds number  $R_t (= k^2/\nu\epsilon)$  becomes small, and part  $f_2^2$  deviates from 1 only when  $\epsilon$  is the dependent variable of Eq. (3). In this case,  $f_2$  and hence  $f_2^2$  have to approach the wall as  $y^m$  with  $m \geq 2$  to keep the sink term finite at the wall. One suggestion due to Hanjalic and Launder<sup>7</sup> (HL) is to take  $f_2^2 = \tilde{\epsilon}/\epsilon$ , with  $\tilde{\epsilon} = \epsilon - 2\nu(\sqrt{k}_{,y})^2$ . The functions and terms  $D$  and  $E$  of two of the more established models, namely, the Launder-Sharma<sup>8</sup> (LS) and the Lam-Bremhorst<sup>9</sup> (LB) models, and of the recently proposed model of Michelassi and Shih<sup>10</sup> (MS) as well as the model constants are compiled in Ref. 6.

### Original DNS-Based RM Model

The model proposed by Rodi and Mansour<sup>2</sup> on the basis of DNS data also fits into the general form of Eqs. (1-3), and the functions and extra terms are given in Table 1. The constants are  $(c_\mu, c_{\epsilon 1}, c_{\epsilon 2}, \sigma_k, \sigma_\epsilon) = (0.09, 1.44, 1.92, 1.3, 1.3)$ . The  $f_\mu$  function was determined by fitting Kim's<sup>4</sup> DNS data for channel flow at  $Re_\tau = 395$ . The form of the modeled  $\epsilon$  equation was derived by evaluating the individual terms in the exact  $\epsilon$  equation from the DNS data for channel flow. At high Reynolds numbers the  $\epsilon$  budget is dominated by the production due to interaction of turbulent fluctuations  $P_\epsilon^4$  and by destruction  $T$ , and their difference is generally modeled as

$$P_\epsilon^4 - T = c_{\epsilon 1} P_k - c_{\epsilon 2} \frac{\epsilon^2}{k} \quad (5)$$

However, near the wall, further generation terms involving mean velocity derivatives can also be influential. In the past, these near-wall effects were simulated by multiplying the terms on the right-hand side of Eq. (5) by empirical functions and/or by adding extra production terms [see Eq. (3)]. However, the physical realism of these functions and extra terms could not be assessed as no data were available. RM noted that near the wall the destruction term  $T$  adjusts to the extra near-wall production and over-reacts so that the net effect is actually an increase in destruction. RM accounted for this combined effect by multiplying the sink term in Eq. (5) by the function  $f_3$  in Table 1, where the argument  $R_p$  is the ratio of the time scale of the dissipating motion to the time scale  $P_k/k$  involving the production of turbulence. The sink term in Eq. (5) needs to be multiplied also by a damping function  $f_2^2$  effective only very

**Table 1 Damping functions and extra terms in RM and RMM models**

Model	Code	$D$	$E$	
Rodi-Mansour	RM	$2\nu(\sqrt{k}, y)^2$	$\nu\nu_t(U)_{,yy}^2 + 0.006\nu \frac{k}{\epsilon} k_{,y} U_{,y} U_{,yy}$	$R_t = k^2/(\nu\epsilon)$ $R_y = y\sqrt{k}/\nu$ $R_p = P_k/(k\sqrt{C_\mu\epsilon/\nu})$ $y^+ = U_\tau y/\nu$
Rodi-Mansour modified	RMM	$\epsilon \exp(-0.095 R_y)$	$\underbrace{1.2\nu\nu_t(U)_{,yy}^2}_{P_\epsilon^{31}} + \underbrace{0.0075\nu \frac{k}{\epsilon} k_{,y} U_{,y} U_{,yy}}_{P_\epsilon^{32}}$	

Model	$f_\mu$	$f_1$	$f_2^1$	$f_2^2$	$f_3$
RM	$[1 - \exp(-0.048 y^+)]^2/[1 + 6\exp(-0.085 y^+)]$	1	$[1 - 0.22\exp(-R_t^2/36)]$	$\bar{\epsilon}/\epsilon$	$\exp(2 R_p^3)$
RMM	$y^+ \leq 100 : [1 - \exp(-2 \cdot 10^{-4} y^+ - 6 \cdot 10^{-4} y^{+2} + 2.5 \cdot 10^{-7} y^{+3})]$ $y^+ \geq 100 : 1$	1	$[1 - 0.22\exp(-0.3357 R_t^{1/2})]$	$\bar{\epsilon}/\epsilon$	$\exp(1.8 R_p^3)$

close to the wall to remain finite at the wall. As the DNS data for the  $\epsilon$  balance were not sufficiently accurate for  $y^+ < 8$ , an  $f_2^2$  function could not be derived from these data and the function  $f_3$  was tuned without its influence. Hence, the effect of the two functions should be separated. The separation can be achieved by writing

$$f_2 = f_2^1 \cdot f_2^2 + f_3 - 1 \quad (6)$$

where  $(f_3 - 1)$  should approach zero faster at the wall than  $f_2^2$ . For other models,  $f_3 = 1$ , and relation (4) is recovered. For the first calculations with the RM model, the  $f_2^2$  function suggested by HL,  $f_2^2 = \bar{\epsilon}/\epsilon = 1 - 2\nu(\sqrt{k}, y)^2/\epsilon$  was taken. For  $f_2^1$ , the exponential function of HL was also adopted. The near-wall production term  $P_\epsilon^3$  involving the second velocity derivative  $U_{,yy}$  was modeled separately by RM and is included as source term  $E$  (see Table 1). This model consists of the two parts  $P_\epsilon^{31}$  and  $P_\epsilon^{32}$ . The part  $P_\epsilon^{31}$  corresponds to the term  $E$  in the LS model and is always positive.  $P_\epsilon^{32}$  makes the  $P_\epsilon^3$  term negative near the wall as was observed from the DNS data. So et al.<sup>11</sup> also have recently proposed a model for simulating the near-wall effects on  $\epsilon$ . Based on Shima's coincidence condition they derived an extra term  $E$  in the  $\epsilon$  equation that is a function of  $\epsilon^*/(\epsilon\bar{\epsilon})$ , where  $\epsilon^* = \epsilon - 2\nu k/y^2$ , and is multiplied by a damping function that ensures  $E$  will vanish away from walls. In applications to flat-plate boundary layers, So et al.<sup>11</sup> have shown that their model predicts the correct shape of the  $\epsilon$  distribution near the wall, but the wall value of  $\epsilon$  is underpredicted by 20%.

Calculations have been performed with the original RM model as given by Eqs. (1-3) and the functions and extra terms in Table 1 for developed channel flow at  $Re_\tau = 395$ . In particular, the HL definition of  $\bar{\epsilon}$  was used. The results show generally satisfactory agreement with the DNS data of Kim<sup>4</sup> with a slight overestimation of both the centerline value of the mean velocity and turbulent kinetic energy, but the dissipation rate  $\epsilon$  is underpredicted in the near-wall region<sup>6</sup> ( $y^+ < 8$ ). Closer examination of the  $\epsilon$  behavior near the wall revealed that the problem is due to the  $\bar{\epsilon}$  distribution and that  $\bar{\epsilon}$  to be used in the destruction term of the  $\epsilon$  equation should rise more quickly with distance from the wall than is given by the HL expression. Hence, the most natural cure to improve the  $\epsilon$  distribution near the wall appears to be a modification of the definition of  $\bar{\epsilon}$ .

#### Modified Form of the RM Model

Various proposals for  $D$  and hence  $\bar{\epsilon}$  have appeared in the literature,<sup>1,10</sup> but none of these produced a satisfactory distribution of  $\epsilon$  when used in combination with the RM model. Hence, alternative forms of  $\bar{\epsilon}$  were investigated, and the following expression for  $\bar{\epsilon}$ , which is of  $\mathcal{O}(y^2)$  at the wall, was found to produce the best overall results:

$$\bar{\epsilon} = \epsilon[1 - \exp(-0.095 \cdot R_y)] \quad (7)$$

with  $R_y = (y\sqrt{k})/\nu$ . The  $f_2^1$  function proposed by HL was replaced by that proposed by Coleman and Mansour<sup>12</sup> (see

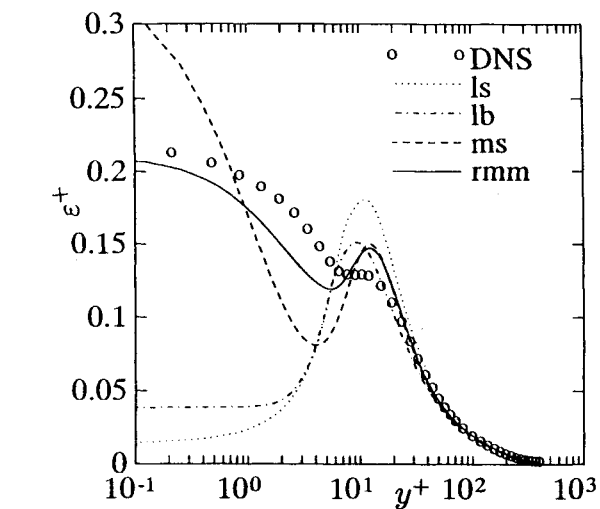
Table 1), since the latter shows a closer agreement to DNS than the former. Since the damping function  $f_\mu$  depends on the definition of  $\bar{\epsilon}$ , the use of a different  $\bar{\epsilon}$  definition also requires a somewhat different  $f_\mu$  function. The retuned form that fits the DNS data with the new  $\bar{\epsilon}$  definition is given in Table 1. This  $f_\mu$  function is compared with various other  $f_\mu$  functions, including that resulting from the DNS data in Ref. 6. The comparison shows that the new  $f_\mu$  function is a good fit to the DNS data. The wall boundary condition for  $\epsilon$  used in connection with the RM and the modified RM model (RMM) model is to put  $\epsilon_w = 2\nu(\sqrt{k}, y)^2$ .

### III. Discussion of Results

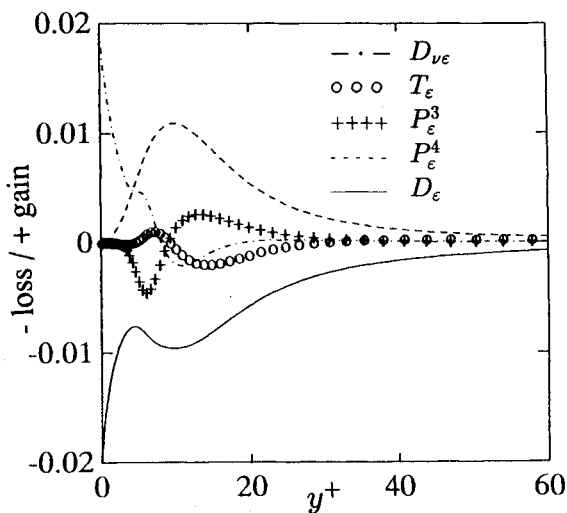
The RMM model was applied to calculate developed channel flow at  $Re_\tau = 180$  and 395 and boundary-layer flow at  $Re_\theta = 670$  and 1410, for which DNS data are available.<sup>3-5</sup> For comparison, these cases were also calculated with the LS, LB, and MS model versions. Note that the former two have been tuned before the availability of DNS data, whereas the MS model was tuned with the aid of the DNS data for the  $Re_\tau = 180$  channel flow. The MS model is included here because it was found to simulate channel flow particularly well and, in contrast to most other models, yields a negative slope of  $\epsilon$  at the wall as observed from the DNS data. Only a few selected results for the higher  $Re$  cases can be presented here; the complete results can be found in Ref. 6.

#### Developed Channel Flow at $Re_\tau = 395$

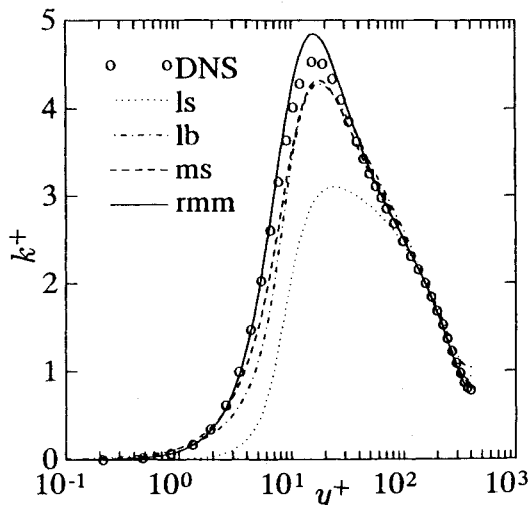
For the channel flow, the numerical calculations were performed by using a simplified form of Michelassi's<sup>13</sup> implicit finite difference algorithm. Ninety-one grid points were placed across the channel with the necessary clustering in the wall region. The  $\epsilon$  profiles predicted by the various models are compared with the DNS data in Fig. 1a. The RMM model gives the best agreement near the wall and also for the wall value of  $\epsilon$ , but the up-down behavior around  $y^+ \approx 10$  is overpredicted. This result is even stronger for the MS model, which also yields a too large  $\epsilon$  value at the wall but still has generally the correct trend. On the other hand, the older LS and LB models give an  $\epsilon$  distribution that is at variance with the DNS data, and they grossly underpredict the wall value of  $\epsilon$  ( $\epsilon^+ \approx 0.22$  according to DNS). The dip in  $\epsilon$  predicted by the RMM model at  $y^+ \approx 6$  is due to the combined effect of the function  $f_3$  and the extra term  $P_\epsilon^{32}$ , both of which act to reduce  $\epsilon$  in this region. However,  $P_\epsilon^{32}$ , which is negative, is overpredicted,<sup>6</sup> leading to the excessive dip. Figure 1b shows the  $\epsilon$  budget, i.e., the individual terms in the modeled  $\epsilon$  Eq. (3) according to the RMM model. The near-wall behavior is now realistic, which was not the case for the original RM model<sup>6</sup>: both diffusion  $Diff_\epsilon$  and destruction  $D_\epsilon$  tend to a fairly large, finite value at the wall, where they balance each other. The modification in the  $\bar{\epsilon}$  formulation has caused the desired increase in the destruction  $D_\epsilon$  absent in the original RM model. For the velocity profiles in wall coordinates three of the models (RMM, LB, and MS) give nearly indistinguishable results, all being in good agreement with the DNS profile.<sup>6</sup> Only the



a) Profile of dissipation rate  $\epsilon$



b)  $\epsilon$  budget predicted with RMM model; terms in Eq. (3) with  $\text{Diff}_\epsilon = D_{\nu\epsilon} + T_\epsilon$



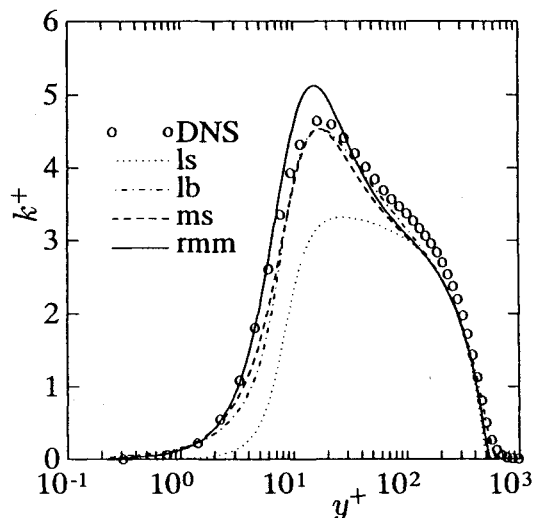
c) Profile of turbulent kinetic energy  $k$

Fig. 1 Channel flow at  $Re_\tau = 395$ .

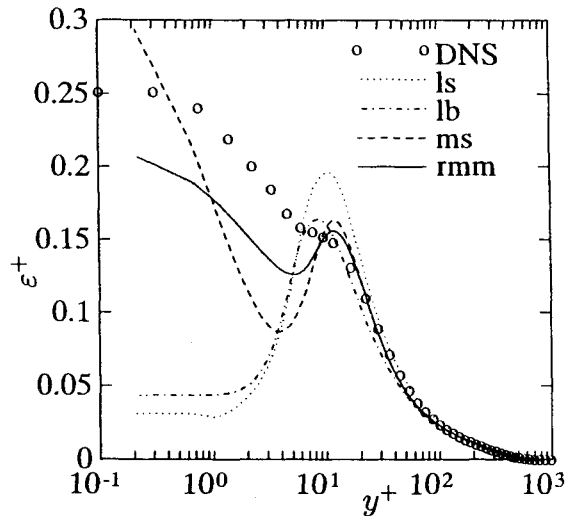
LS model overpredicts the velocity in the central part of the channel. This result can be traced to  $f_\mu$  used by LS, which was found not to reach unity for  $y^+ \geq 100$ , but to attain values of 0.90–0.95. Differences in the predicted shear stress  $\bar{uv}$  between the models can only be detected very near the wall<sup>6</sup> ( $y^+ < 10$ ). The RMM model is closest to the DNS data, the MS predic-

tions are only slightly lower, whereas both LS and LB underpredict the shear stress there to a larger extent.

The profiles of  $k$  are compared in Fig. 1c. Again, the RMM and MS models produce the best agreement with the DNS data, but the RMM model predicts the  $k$  peak somewhat too high, and the MS model underpredicts the peak of  $k$  slightly. The LS model does a fairly poor job in predicting the  $k$  profile as the  $k$  level in the near-wall channel region is considerably too low, probably because of the inappropriate damping function  $f_\mu$  used. The LB model prediction is similar to that resulting from the MS model, but in the range  $0 < y^+ < 10$  the growth rate is more severely underpredicted. The growth rate very close to the wall, where  $k^+ = c_k y^{+2}$ , is of particular interest because it is related to the dissipation rate at the wall (in fact  $\epsilon_w^+ = 2c_k$ ). The  $c_k$  values predicted by the LS, MS, and RMM models are, respectively, 0.01, 0.14, and 0.10. Only the RMM model is nearly correct. For channel flow at  $Re_\tau = 180$



a) Profile of turbulent kinetic energy  $k$



b) Profile of dissipation rate  $\epsilon$

Fig. 2 Boundary layer at  $Re_\theta = 1410$ .

Table 2 Boundary-layer integral parameters

	$Re_\theta = 670$		$Re_\theta = 1400$	
	$c_f \times 10^3$	$H$	$c_f \times 10^3$	$H$
DNS	4.86	1.50	4.14	1.43
LS	4.02	1.56	3.55	1.43
LB	4.77	1.48	4.18	1.39
MS	4.52	1.50	3.92	1.41
RMM	4.88	1.49	4.13	1.41

generally the same behavior can be observed as for the higher Reynolds number case, so that the same remarks apply.<sup>6</sup>

#### Boundary-Layer Flow

The boundary-layer flow was calculated with an elliptic finite-volume procedure<sup>14</sup> using 122 nonuniformly spaced grid points across the layer (for further details see Ref. 6). The calculation domain covered a streamwise distance  $x$  such that  $Re_\theta = 300$  at the inflow and  $Re_\theta = 1410$  at the outflow boundary. Table 2 compares for the two  $x$  positions, where the momentum-thickness Reynolds number  $Re_\theta$  is 670 and 1410, the friction coefficient  $c_f$  and shape parameter  $H$  predicted by the various models with the DNS data. At both Reynolds numbers, the new model gives the best overall agreement. In particular, the  $c_f$  value predicted by the RMM model is considerably closer to the data than  $c_f$  predicted by any other model. For the profiles of  $U$ ,  $\overline{uv}$ ,  $k$ , and  $\epsilon$ , basically the same behavior can be observed as for the channel flow. The LS model predicts too high a velocity in the outer region of the boundary layer, but for this flow the MS model results are also slightly too high (in the intermediate region), whereas the LB and RMM models yield very good agreement with the DNS profile.<sup>6</sup> Very near the wall, the  $\overline{uv}$  distribution is again predicted best by the RMM model, a result that explains the superior prediction of the  $c_f$  values. But near the boundary-layer edge, all models except the LB model yield too fast an approach of the shear stress to zero.<sup>6</sup> Concerning the  $k$  distribution (Fig. 2a), the new model is again the most accurate one near the wall. But also in the boundary-layer case it predicts a somewhat excessive  $k$  peak, whereas the LB and MS models reproduce the peak value correctly. At the boundary-layer edge, the LB model predicts the approach of  $k$  to zero correctly, whereas all of the other models predict too fast an approach. The  $\epsilon$  distribution resulting from the RMM model (Fig. 2b) is very close to the one for the channel flow shown in Fig. 1a. On the other hand, the DNS data show somewhat larger  $\epsilon$  values very near the wall for the boundary layer than for the channel flow, and hence the agreement is not as good as in the channel flow case. However, the  $\epsilon$  prediction by the RMM model is still by far the best. Virtually the same remarks can be made on the calculations of the  $Re_\theta = 670$  boundary layer.<sup>6</sup>

All of the results have been checked for grid independence by performing calculations on different grids. It was found that grid independence in the critical near-wall region requires the first grid point to be placed at  $y^+ = 0.5 - 1$ . Use of fewer than 61 grid points in the normal direction with fewer than 20 points in the region  $0 < y^+ < 100$  led to a rapid deterioration of the results. In particular,  $\epsilon_w$  was found to be sensitive to the number of grid points placed within the buffer layer.

#### IV. Conclusions

The low  $Re$   $k$ - $\epsilon$  model proposed by Rodi and Mansour<sup>2</sup> on the basis of DNS data was complemented by a damping function multiplying the destruction term in the model  $\epsilon$  equation. First a function involving  $\tilde{\epsilon}$  as defined by Hanjalic and Launder<sup>7</sup> was tried. Very near the wall, this method led to an underprediction of  $\epsilon$  and to an unrealistic  $\epsilon$  balance. A different definition of  $\tilde{\epsilon}$  was therefore introduced, and some of the constants in the RM model were retuned. The resulting modified version (RMM) yielded generally good predictions of all major quantities in developed channel and boundary-layer flows compared with the DNS data. The model mimics correctly the change in sign of the near-wall production  $P_\epsilon^3$ , which in turn is mainly responsible for the fairly realistic simulation of the  $\epsilon$  distribution near the wall. However, the model produces some excessive up-down behavior of  $\epsilon$  in this region and requires further fine tuning of the constants. Also, the model has to be tested in the future for other flow situations.

#### References

<sup>1</sup>Patel, V. C., Rodi, W., and Scheuerer, G., "Turbulence Models for Near-Wall and Low-Reynolds Number Flows: A Review," *AIAA*

*Journal*, Vol. 23, 1985, pp. 1308-1319.

<sup>2</sup>Rodi, W., and Mansour, N. N., "Low-Reynolds Number  $k$ - $\epsilon$  Modeling with the Aid of Direct Simulation Data," *Journal of Fluid Mechanics*, Vol. 250, 1993, pp. 509-529.

<sup>3</sup>Kim, J., Moin, P., and Moser, R., "Turbulence Statistics in Fully Developed Channel Flow at Low Reynolds Number," *Journal of Fluid Mechanics*, Vol. 177, 1987, pp. 133-166.

<sup>4</sup>Kim, J., private communication, NASA Ames Research Center, 1990.

<sup>5</sup>Spalart, P. R., "Direct Simulation of a Turbulent Boundary Layer up to  $Re_\theta = 1410$ ," *Journal of Fluid Mechanics*, Vol. 187, 1988, pp. 61-98.

<sup>6</sup>Michelassi, V., Rodi, W., and Zhu, J., "Testing a Low Reynolds Number  $k$ - $\epsilon$  Turbulence Model Based on Direct Simulation Data," Univ. of Karlsruhe, Rept. SFB 210/T/83, Karlsruhe, Germany, Dec. 1992.

<sup>7</sup>Hanjalic, K., and Launder, B. E., "Contribution Towards a Reynolds-Stress Closure for Low-Reynolds Number Turbulence," *Journal of Fluid Mechanics*, Vol. 74, 1976, pp. 593-610.

<sup>8</sup>Launder, B. E., and Sharma, B. I., "Application of the Energy-dissipation Model of Turbulence to the Calculation of Flow near a Spinning Disc," *Letters in Heat and Mass Transfer*, Vol. 1, 1974, pp. 131-138.

<sup>9</sup>Lam, C. K. G., and Bremhorst, K. A., "Modified Form of the  $k$ - $\epsilon$  Model for Predicting Wall Turbulence," *Journal of Fluids Engineering*, Vol. 103, 1981, pp. 456-460.

<sup>10</sup>Michelassi, V., and Shih, T. H., "Low Reynolds Number Two-Equation Modelling of Turbulent Flows," NASA TM-104368, May 1991.

<sup>11</sup>So, R. M. C., Zhang, H. S., and Speziale, C. G., "Near-Wall Modeling of the Dissipation Rate Equation," *AIAA Journal*, Vol. 29, 1991, pp. 2069-2076.

<sup>12</sup>Coleman, G. N., and Mansour, N. N., "Simulation and Modeling of Homogeneous Compressible Turbulence Under Isotropic Mean Compression," *Proceedings of the 8th Turbulent Shear Flows Symposium*, Munich, Germany, Sept. 9-11, 1991, pp. 21-3-1-21-3-6.

<sup>13</sup>Michelassi, V., "Testing of Turbulence Models by an Artificial Compressibility Solution Method," Univ. of Karlsruhe, Rept. SFB 210/T/49, Karlsruhe, Germany, 1988.

<sup>14</sup>Rodi, W., Majumdar, S., and Schönung, B., "Finite-Volume Methods for Two-Dimensional Incompressible Flows with Complex Boundaries," *Computational Methods in Applied Mechanics and Engineering*, Vol. 75, 1989, pp. 369-392.

## Evaluation of Baldwin-Barth Turbulence Model with an Axisymmetric Afterbody-Exhaust Jet Flowfield

M. Kandula\*

Lockheed Engineering and Sciences Company,  
Houston, Texas 77058

and

P. G. Buning†

NASA Ames Research Center,  
Moffett Field, California 94035

#### Nomenclature

$c_p$	= pressure coefficient
$D_{\max}$	= maximum body diameter
$k$	= turbulent kinetic energy
$M$	= Mach number

Received Nov. 6, 1992; presented as Paper 93-0418 at the AIAA 31st Aerospace Sciences Meeting, Reno, NV, Jan. 11-14, 1993; revision received March 1, 1993; accepted for publication March 2, 1993. Copyright © 1993 by the American Institute of Aeronautics and Astronautics, Inc. No copyright is asserted in the United States under Title 17, U.S. Code. The U.S. Government has a royalty-free license to exercise all rights under the copyright claimed herein for Governmental purposes. All other rights are reserved by the copyright owner.

\*Group Leader, Computational Fluid Dynamics. Senior Member AIAA.

†Research Scientist. Senior Member AIAA.